Conductance Oscillations in Squashed Carbon Nanotubes

A. Svizhenko, H. Mehrez, and M. P. Anantram
Mail Stop: 229-1, NASA Ames Research center, Moffett Field, CA 94035-1000, USA
(Dated: December 10, 2003)

A combination of molecular dynamics and electrical conductance calculations are used to probe the electromechanical properties of squashed metallic carbon nanotubes. We find that the conductance and bandgap of armchair nanotubes show oscillations upon squashing. The physical origin of these oscillations is attributed to interaction of carbon atoms with a fourth neighbor. Squashing of armchair and zigzag nanotubes ultimately leads to metallic behavior.

Experiments probing the electromechanical response of carbon nanotubes have been the most interesting recent work in nanotubes.[1–5] These experiments involve nanotubes interacting electrically with contacts and mechanically with an atomic force microscope (AFM) tip. Apart from the fundamental physics governing the electromechanical response, these experiments are also important to the future use of carbon nanotubes in actuators and nano electromechanical devices.[6] There are two categories of experiments exploring the electromechanical properties: one which involves and the second which does not involve, a change in the nanotube length.[7] The first experiment in category one involved deforming a nanotube suspended in a silicon dioxide trench by an atomic force microscope (AFM) tip.[2] The electrical conductance was found to decrease by two orders of magnitude upon modest deformation. Subsequent modeling[8] showed that the primary reason for conductance change is a strain induced bandgap due to bond stretching in the axial direction. More recent experiments have also observed a chirality dependent change in bandgap upon axial strain,[3,4] consistent with earlier theoretical work.[9,10]

The second class of experiments on electromechanical response involve the squashing of nanotubes lying on a hard substrate[1,5]. We believe that in these experiments, the physics is determined by curvature effects and the interaction of carbon atoms with a fourth neighbor. The change in nanotube length, if any, will only play a secondary role. Theoretical work has shown that squashing of metallic zigzag nanotubes leads to the closing of the curvature induced gap[12–14]. On the other hand, it has been predicted that while armchair nanotubes develop a bandgap upon squashing[12–15], chiral nanotubes are insensitive to squashing because of a large wave vector mismatch of isoenergetic states.[13]

The purpose of this letter is to investigate the electromechanical properties of squashed single wall armchair and zigzag nanotubes lying on a substrate. We present a unified picture of the underlying physics from the undeformed to the well deformed cases. Our central result is that novel bandgap and conductance oscillations emerge with squashing. The bandgap oscillations are discussed in term of the following factors: **(A)** curvature effects within the three nearest neighbor graphene frame work, **(B)** interaction with a fourth neighbor between atoms at the edge of the nanotube (Fig. 1) and **(C)** interaction with a fourth neighbor between atoms at the top and bottom of the nanotube (Fig. 1). The transition region between regions **(A)**, **(B)** and **(C)** leads to oscillations in the bandgap of armchair nanotubes.

We consider a (12,0) zigzag and (6,6) armchair metallic carbon nanotube, which have 48 and 24 atoms per unit cell respectively. Their diameters of 9.4 $\AA$ (12,0) and 8.14 $\AA$ (6,6) are similar. To model the squashing of nanotubes we note that typical AFMs have a tip diameter that is larger than 25 nm, and that the diameter of single wall nanotubes is typically 2 nm or smaller. The carbon nanotubes were squashed using graphene sheets of a much larger dimension to mimic deformation with a large diameter AFM tip. So as to focus on the interaction between nanotube atoms, we kept the atoms in the graphene layers fixed. Molecular dynamics simulations were performed using the density functional theory based tight binding (DFTB) method.[18] The distance between the graphene sheets varied from approximately 18 $\AA$ to 6 $\AA$, with increasing deformation. Zigzag nanotubes have three configurations (Fig. 1,a-c). First the nanotube is symmetric, with top atoms facing bottom atoms (Fig. 1,a). At higher deformation, top atoms perform a 'tank-treading' motion to face hollow sites on the bottom, which corresponds to the second configuration (Fig. 1,b). Finally, the tube suffers a shear deformation along the axis, which tilts the planes of nanotube rings, and transits to the third configuration (Fig. 1,c). The armchair nanotube shows a slow gradual 'tank-treading' motion of top atoms, which tend to face hollow sites on the bottom (Fig. 1,d-f). The bandgap and conductance of these deformed nanotubes are calculated using the same self-consistent non orthogonal tight binding parameterization of reference [18].

We will first discuss the bandgap change in the case of metallic zigzag nanotubes. The bandgap as a function of the distance between the top and bottom of the nanotube (d) is shown in Fig. 2. Undeformed (12,0) zigzag carbon nanotubes have a curvature induced bandgap ($\sim$ 200 meV).[21] This bandgap arises due to the curvature effect which makes hopping along the axial and angular bonds inequivalent. Upon squashing, the axial and angular bonds become equivalent at the top and bottom of the nanotube but become more inequivalent at the edges. The net effect is to further decrease the curvature induced bandgap. With further deformation, at

$d < 6\mathring{A}$, the bandgap decreases more rapidly. Finally at $d \sim 5\mathring{A}$ the bandgap closes and the zigzag nanotube becomes metallic, which agrees with the results of references 12 and 14. The physics in the regime, $d > 6\mathring{A}$ can be understood within the three interacting neighbor picture of carbon nanotubes[21] (factor **A**). We find that the bandgap decrease and closure at $d < 6\mathring{A}$ is because atoms at the edge interact with a *fourth* neighbor (factor **B**). Further, we find that the interaction with the fourth neighbor always lie in pairs: for every interaction of atoms belonging to the same graphene sublattice A (type AA) there is an interaction of type BB, between atoms belonging to the sublattice B, with the same strength. This is due to the fact that under the mirror symmetry operation of the zigzag nanotubes around a plane perpendicular to the axis, atoms A will be transformed into atoms B and vice versa. These interactions always couple atoms in the same ring and are the strongest at the edges although the calculation included coupling between all atoms within a cut-off radius of 4.2 $\mathring{A}$. The bandgap closing at $d \sim 5\mathring{A}$ is now explained using a degenerate perturbation theory involving only the crossing subbands in the π orbital picture. The two pairs of crossing subbands are represented by (π_1, π_1^*) and (π_2,π_2^*), where π_i and π_i^* correspond to the bonding and antibonding states respectively. The interaction between the crossing subbands can be written as,

$$V_{\pi_i,\pi_j} = V^{AA}_{\pi_i,\pi_j} + V^{BB}_{\pi_i,\pi_j} + V^{AB}_{\pi_i,\pi_j} + V^{BA}_{\pi_i,\pi_j} \quad (1)$$

$$V_{\pi_i,\pi_j^*} = V^{AA}_{\pi_i,\pi_j^*} + V^{BB}_{\pi_i,\pi_j^*} + V^{AB}_{\pi_i,\pi_j^*} + V^{BA}_{\pi_i,\pi_j^*}, \quad (2)$$

where $i, j \in 1, 2$. There are two important features in the relative values of the terms in Eqs. (1) and (2). First, the distance between atoms A and B is larger than that between two atoms, both of type A or type B. So, we can neglect interactions involving AB. Second, within the π orbital wave functions,

$$V^{AA}_{\pi_i\pi_j} = V^{BB}_{\pi_i\pi_j},\ V^{AA}_{\pi_i^*\pi_j^*} = V^{BB}_{\pi_i^*\pi_j^*} \text{ and} \quad (3)$$

$$V^{AA}_{\pi_i\pi_j^*} = -V^{BB}_{\pi_i\pi_j^*}, \text{ when } l_{AA} = l_{BB}, \quad (4)$$

where l_{AA} and l_{BB} are the distances between AA and BB. Using Eqs. (1) - (4), the perturbation Hamiltonian arising from the four degenerate levels at k=0 can then be written as,

$$H = \begin{pmatrix} V_{\pi_1\pi_1} & 0 & V_{\pi_1\pi_2} & 0 \\ 0 & V_{\pi_1\pi_1} & 0 & V_{\pi_1\pi_2} \\ V^*_{\pi_1\pi_2} & 0 & V_{\pi_2\pi_2} & 0 \\ 0 & V^*_{\pi_1\pi_2} & 0 & V_{\pi_2\pi_2} \end{pmatrix}, \quad (5)$$

where the four rows/columns numbered 1, 2, 3 and 4 correspond to π_1, π_1^*, π_2 and π_2^* respectively. The main feature of H in Eq. (5) is that the bonding states of one pair do not interact with the antibonding states of the other pair of crossing subbands. The main non zero interaction is between the π_1 and π_2 bands, and between the π_1^* and π_2^* bands. As a result, H lifts the degeneracy only between the two pairs of crossing subbands, shifting them by energy $(V_{\pi_1\pi_1} \pm |V_{\pi_1\pi_2}|)$, without perturbing the bonding-antibonding states within each pair. Thus a bonding state of one pair crosses the antibonding state of the other pair without a bandgap and the crossing point corresponds to the new Fermi energy. This simple π-orbital analysis is in excellent agreement with the four orbital results, as shown in Fig. 3 (a). Note, that the curvature induced splitting between π and π^* bands of each pair is still present in the bandstructure, but no longer affects the conductance of the tube.

The inset of Fig. 2 shows that number of modes at the Fermi energy can be larger than two at high deformation. As a result, the conductance can be larger than $4e^2/h$, which is the theoretical maximum for the undeformed nanotube. This region cannot be understood within the π orbital picture and is a result of our four orbital calculations. A typical band structure in this region is shown in Fig. 3(b).

We will now discuss our results for the bandgap and conductance change of armchair nanotubes. The bandgap of armchair nanotubes is nearly zero for $d > 6\mathring{A}$ and begins to increase for $d < 6\mathring{A}$. This is the approximate d at which the bandgap of a zigzag nanotube with a similar diameter closes. Note that while the effect of curvature with only three nearest neighbors induces a bandgap change in zigzag nanotubes, it causes very little change in the case of armchair nanotubes. Further, while interaction with a fourth neighbor which become important as d becomes smaller than 6 $\mathring{A}$ causes the bandgap to close for zigzag nanotubes, it causes an opening of the bandgap in armchair nanotubes.

The prevalence or cancellation of certain types of fourth neighbor interaction is the underlying physics of the dramatic bandgap oscillations shown in Fig. 4. The Hamiltonian for the interaction between the π and π^* crossing subbands of an armchair nanotube at $k = \pm\frac{2\pi}{3a_0}$ is,[21–23]

$$H = \begin{pmatrix} V_{\pi\pi} & V_{\pi\pi^*} \\ V_{\pi^*\pi} & V_{\pi^*\pi^*} \end{pmatrix}, \quad (6)$$

where again $V_{\pi\pi}$ and $V_{\pi\pi^*}$ are defined as in Eqs. (1) and (2). From Eq. (6), the crossing subband energies are $(V_{\pi\pi} + V_{\pi^*\pi^*} \pm \sqrt{(V_{\pi\pi} - V_{\pi^*\pi^*})^2 + 4|V_{\pi\pi^*}|^2})/2$, centered at $V_{\pi\pi}$ and split by $2|V_{\pi\pi^*}|$. We have assumed $V_{\pi\pi} \sim V_{\pi^*\pi^*}$, which holds in the case of AA and BB interaction. Upon squashing of an undeformed armchair nanotube, we find that 6 AA and 6 BB interactions become non negligible per unit cell, at the *edges*. These interactions couple atoms in neighboring rings and are shown in Fig. 1 (d). l_{BB} is slightly shorter than l_{AA}, and so the bandgap increases as d decreases from $6\mathring{A}$ (factor **B**). l_{BB} and l_{AA} become comparable upon further deformation. This causes the bandgap to decrease and reach a minimum around $d \sim 2.71\mathring{A}$, when $V^{AA}_{\pi\pi^*} = -V^{BB}_{\pi\pi^*}$. Again, note that while our arguments here use only the strongest interactions, our tight binding calculations consider all interaction between atoms that are closer than

4.2Å. At further deformation, $d < 2.71Å$, l_{AA} becomes shorter than l_{BB} (Fig. 1 (e)) which leads to the second bandgap increase in Fig. 4 (factor **B**).

For $d < 2.5Å$, the deformation is high enough to couple top-bottom atoms of the same ring (factor **C**) in addition to the coupling of atoms at the edges as shown in Fig. 1(e). By analysing the matrix elements, one can show that $V^{AA}_{\pi\pi^*}$(same ring) $= -2V^{AA}_{\pi\pi^*}$(neighboring rings). The interactions at the edges and top-bottom contribute with opposite signs, which leads to a decrease and the second minimum of bandgap at $d \sim 2.5Å$. When $d < 2.5Å$, the interaction between top-bottom atoms dominates over the edge atoms, leading to the third increase in bandgap.

The evolution of the band structure of the armchair nanotube upon deformation is shown in Fig. 5. Note that the deformation causes a shift of the crossing subbands and a monotonic decrease in Fermi energy. When the coupling between top-bottom atoms is strong enough, at $d < 2.32Å$, the bandgap becomes indirect with the valence band corresponding to a non crossing subband while the conduction band is still primarily π^*. Upon further deformation the Fermi energy passes through the non crossing subband, which makes the nanotube metallic. This mixing of crossing and noncrossing subbands is similar to the zigzag case and dominates at all higher deformations until the tube breaks.

In conclusion, we find that interaction with a fourth neighbor at the edges (and not top-bottom) of armchair nanotubes causes a bandgap to open. Interplay between various fourth neighbor interactions at both the edges and top-bottom causes the bandgap to oscillate with deformation. These oscillation are large enough (> 100 meV) to be experimentally observable. The picture developed to explain the oscillatory bandgap of armchair nanotube also serves well in explaining the closure of bandgap in zigzag nanotubes, which arises due to interactions with fourth neighbors at the edges of the deformed nanotube.

[1] S. Paulson et al., Appl. Phys. Lett. **75**, 2936 (1999)
[2] T. W. Tombler et al., Nature **405**, 769 (2000)
[3] E. D. Minot, Y. Yaish, V. Sazonova, J-Y. Park, M. Brink and P. L. McEuen, Phys. Rev. Lett. **90**, 156401 (2003);
[4] J. Cao, Q. Wang and H. Dai, Phys. Rev. Lett. **90**, 157601 (2003)
[5] C. Gomez-Navarro, P. J. DePablo and J. Gomez-Herrero, Accepted in Adv. Mater. (2004)
[6] Yu. N. Gartstein, A. A. Zakhidov, and R. H. Baughman, Phys. Rev. Lett. **89**, 45503 (2002); Phys. Rev. B **68**, 115415 (2003)
[7] Experiments involving torsional strain of the nanotube remain largely unexplored.
[8] A. Maiti, A. Svizhenko, and M. P. Anantram, Phys. Rev. Lett. **88**, 126805 (2002)
[9] R. Heyd, A. Charlier, E. McRae, Phys. Rev. B **55**, 6820 (1997).
[10] L. Yang, M. P. Anantram, J. Han, J. P. Lu, Phys. Rev. B **60**, 13874 (1999)
[11] P. Delaney, H. J. Choi, J. Ihm, S. G. Louie and M. Cohen, Nature, **391**, 466 (1998)
[12] C. J. Park, Y. H. Kim, and K. J. Chang, Phys. Rev. B **60**, 10656 (1999)
[13] P. E. Lammert, P. Zhang and V. H. Crespi, Phys. Rev. Lett. **84**, 2453 (2000)
[14] O. Gülseren, T. Yildirim, S. Ciraci, and Ç. Kiliç, Phys. Rev. B **65**, 155410 (2002)
[15] J.-Q. Lu, J. Wu, W. Duan, F. Liu, B.-F. Zhu and B.-L. Gu, Phys. Rev. Lett. **90**, 156601 (2003)
[16] D. Porezag, T. Frauenheim, T. Kohler, G. Seifert, and R. Kaschner, Phys. Rev. B **51**, 12947 (1995); G. Seifert, D. Porezag, and T. Frauenheim, Int. J. Quantum Chemistry, **58**, 185 (1996).
[17] G. Seifert, T. Kohler, and T. Frauenheim, Appl. Phys. Lett. **77**, 1313, (2000); X. Y. Zhu, S. M. Lee, Y. H. Lee, and T. Frauenheim, Phys. Rev. Lett. **85**, 2757, (2000)
[18] D. Porezag, T. Frauenheim, T. Kohler, G. Seifert, and R. Kaschner, Phys. Rev. B **51**, 12947 (1995); G. Seifert, D. Porezag, and T. Frauenheim, Int. J. Quantum Chemistry **58**, 185 (1996).
[19] M. Elstner, D. Porezag, G. Jungnickel, J. Elsner, M. Haugk, T. Frauenheim, S. Suhai, and G. Seifert, Phys. Rev. B **58**, 7260 (1998).
[21] N. Hamada, S. I. Sawada and A. Oshiyama, Phys. Rev. Lett. **68**, 1579 (1992);
[22] J. W. Mintmire, B. I. Dunlap and C. T. White, Phys. Rev. Lett. **68**, 631 (1992);
[23] R. Saito, M. Fujita, G. Dresselhaus and M. S. Dresselhaus, Appl. Phys. Lett. **60**, 2204 (1992)

FIG. 1: Optimized zigzag (a-c) and armchair (d-f) nanotubes. Graphene layers (not shown) are typically 2.5 $\AA$ above/below the nanotube. Circles and squares denote atoms in different rings. (a),(d) At small deformations, atoms at the edges interact. The bandgap becomes zero when $l_{AA} = l_{BB}$. (b),(e) At medium deformations, interactions between top and bottom atoms compete with edge interactions. (c),(f) Top-bottom interactions prevail at high deformations.

FIG. 2: Bandgap of the (12,0) nanotubes as a function of deformation. The curvature induced bandgap decreases due to flattening of top and bottom of the nanotube. The interaction with a fourth neighbor leads to the bandgap decrease and closure at $d < 5\AA$. The inset shows the conductance as a function of deformation. At high deformations, conductance increases due to new conducting modes near the Fermi energy.

FIG. 3: The sp^3 TB bandstructure of a deformed (12,0) nanotube. (a) The gap closes because the interaction shifts one pair of $\pi - \pi^*$ subbands with respect to the other. The Fermi energy is at the crossing point of π_1 and π_2^*. (b) Very high deformation creates new conducting modes in the vicinity of the Fermi energy.

FIG. 4: Bandgap of the (6,6) nanotubes as a function of deformation. The interaction with a fourth neighbor opens a bandgap at $d \sim 6\AA$. The competition between AA and BB interactions at the edge results in the first minimum at $d \sim 2.71\AA$. The second minimum at $d \sim 2.5\AA$ is due to the cancellation of edge and top-bottom interactions. The final closure of the gap is because of the presence of noncrossing subbands. In the inset, the conductance as a function of deformation shows pronounced oscillations. At higher deformations the number of conducting modes is higher than 2.

FIG. 5: The evolution of the sp^3 TB bandstructure of deformed (6,6) nanotube. (a) The bandgap opens due to to one of the interactions of the edge atoms. (b) The first closure of the gap due to interplay of edge interactions. While the contributions to $V_{\pi\pi^*}$ cancel out, resulting in zero gap, $V_{\pi\pi}$ and $V_{\pi^*\pi^*}$ add up, resulting in a constant shift of the band center / Fermi energy. (c) The cancellation of edge and top-bottom AA interactions. (d) The final closure of the gap due to the overlap of crossing and noncrossing subbands. Note the indirect character of the bandgap.

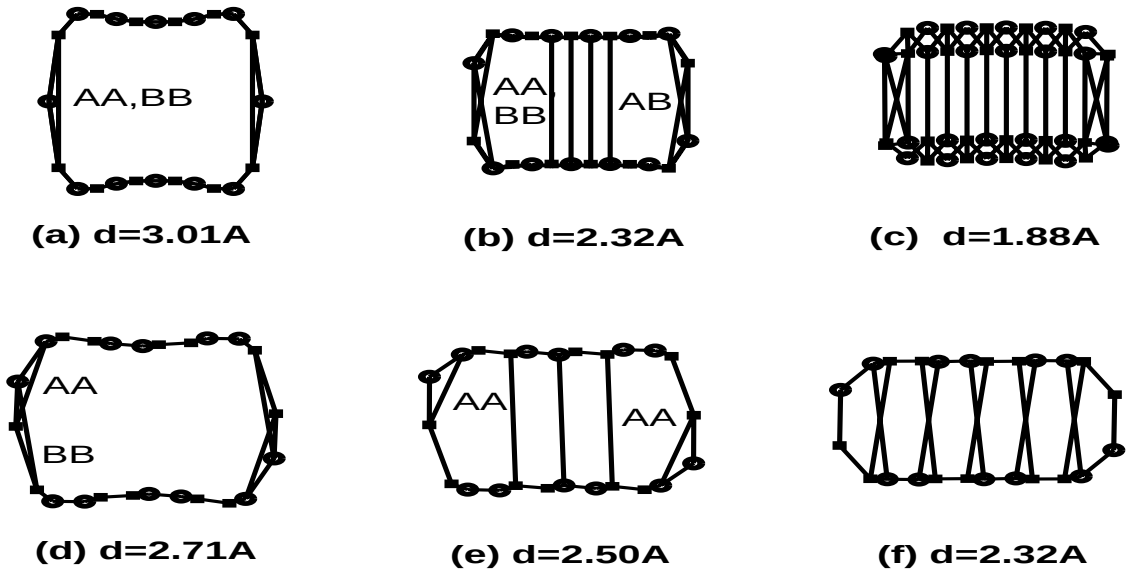

Fig. 1

Svizhenko, Mehrez,Anantram

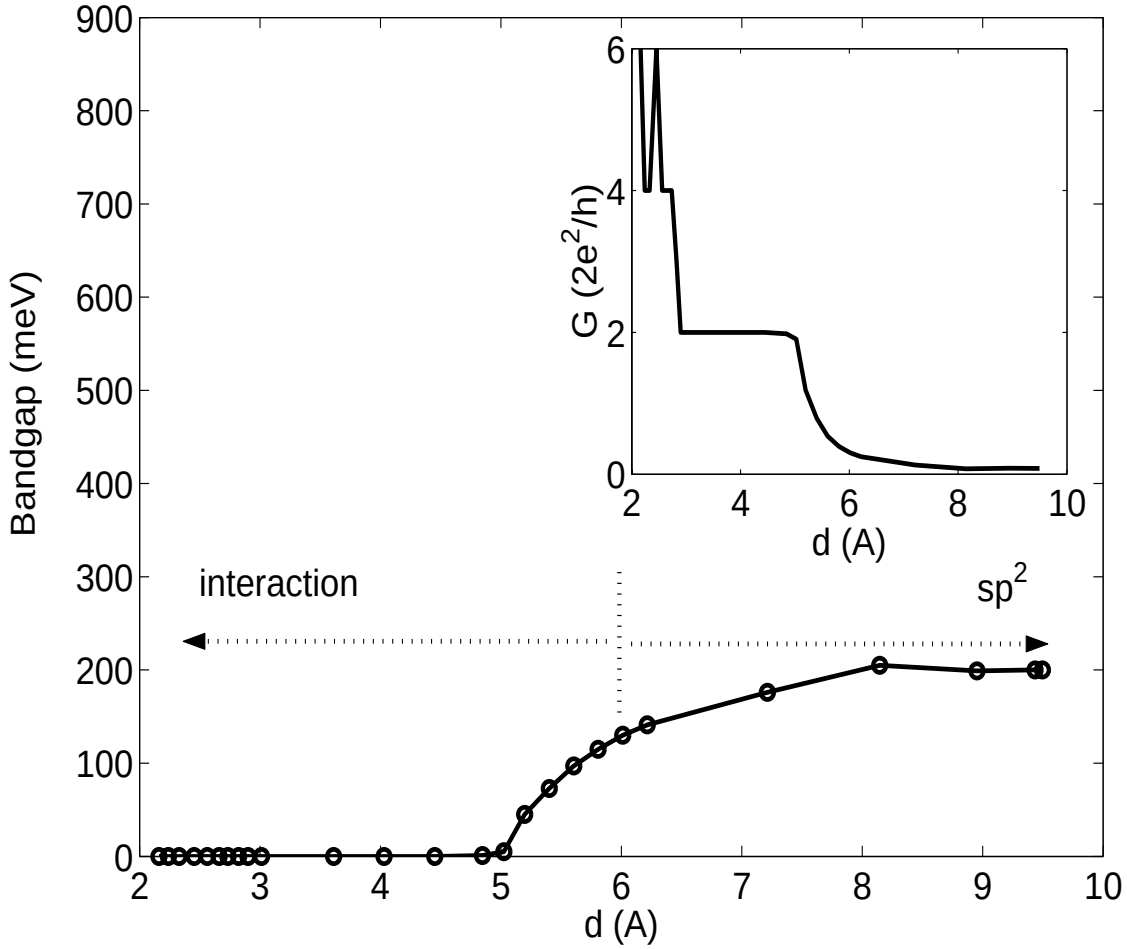

Fig. 2

Svizhenko, Mehrez,Anantram

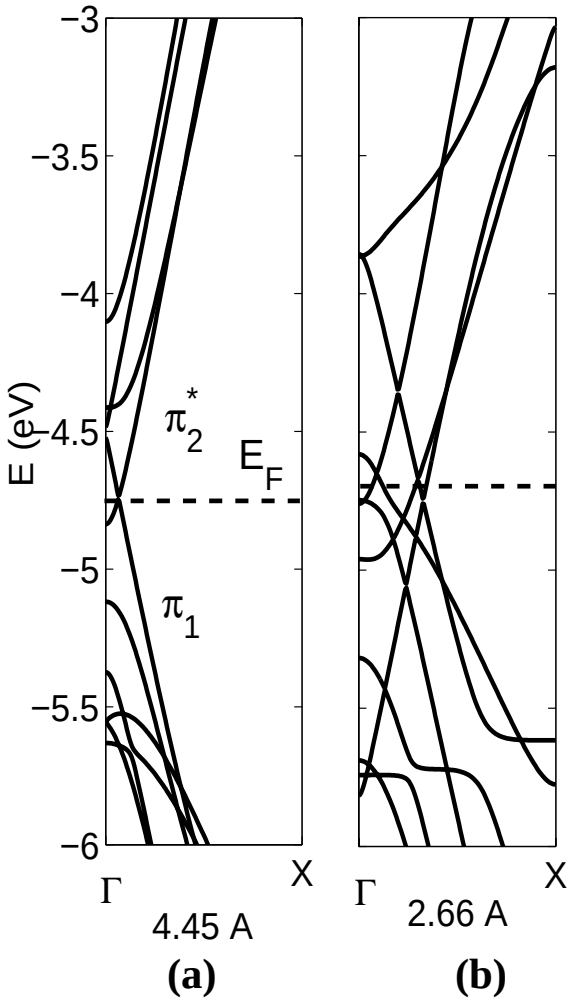

Fig. 3

Svizhenko, Mehrez,Anantram

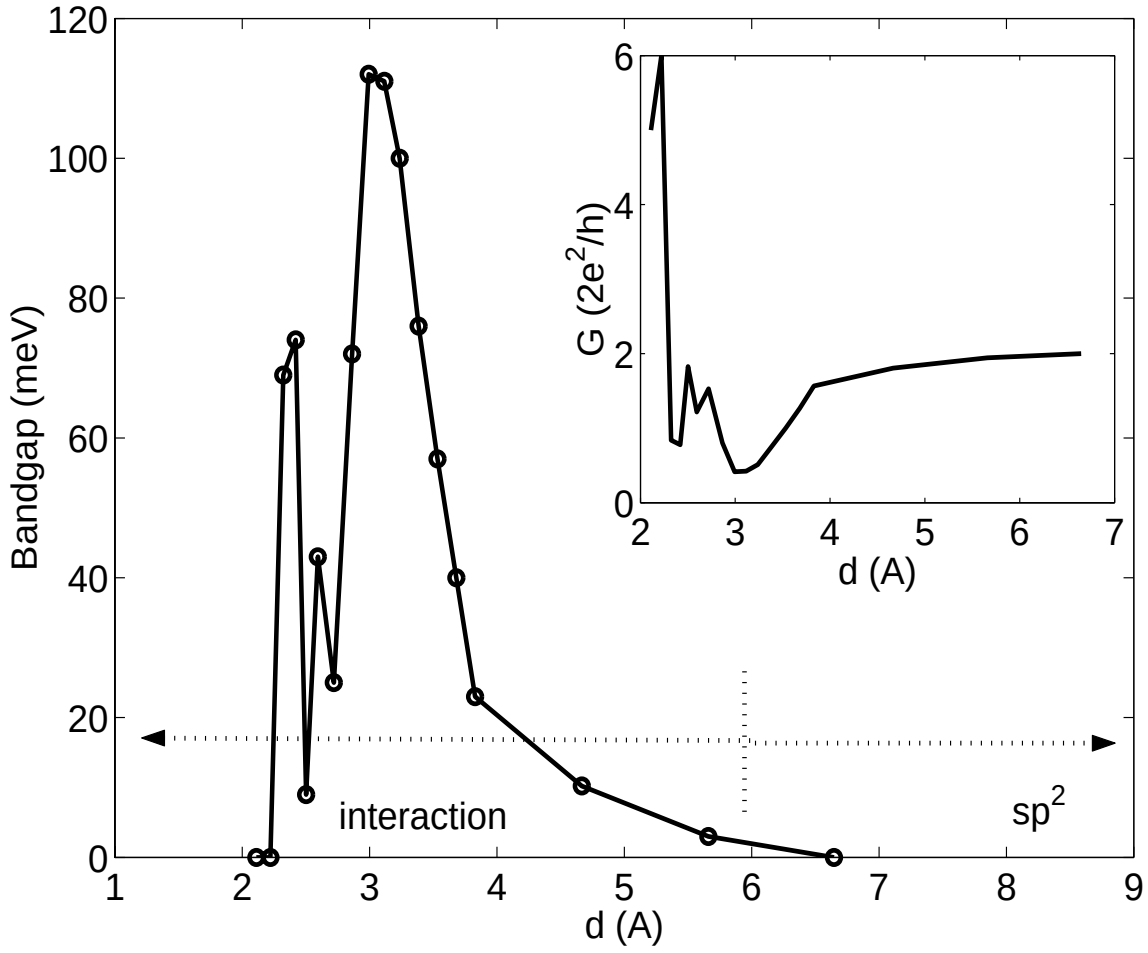

Fig. 4

Svizhenko, Mehrez,Anantram

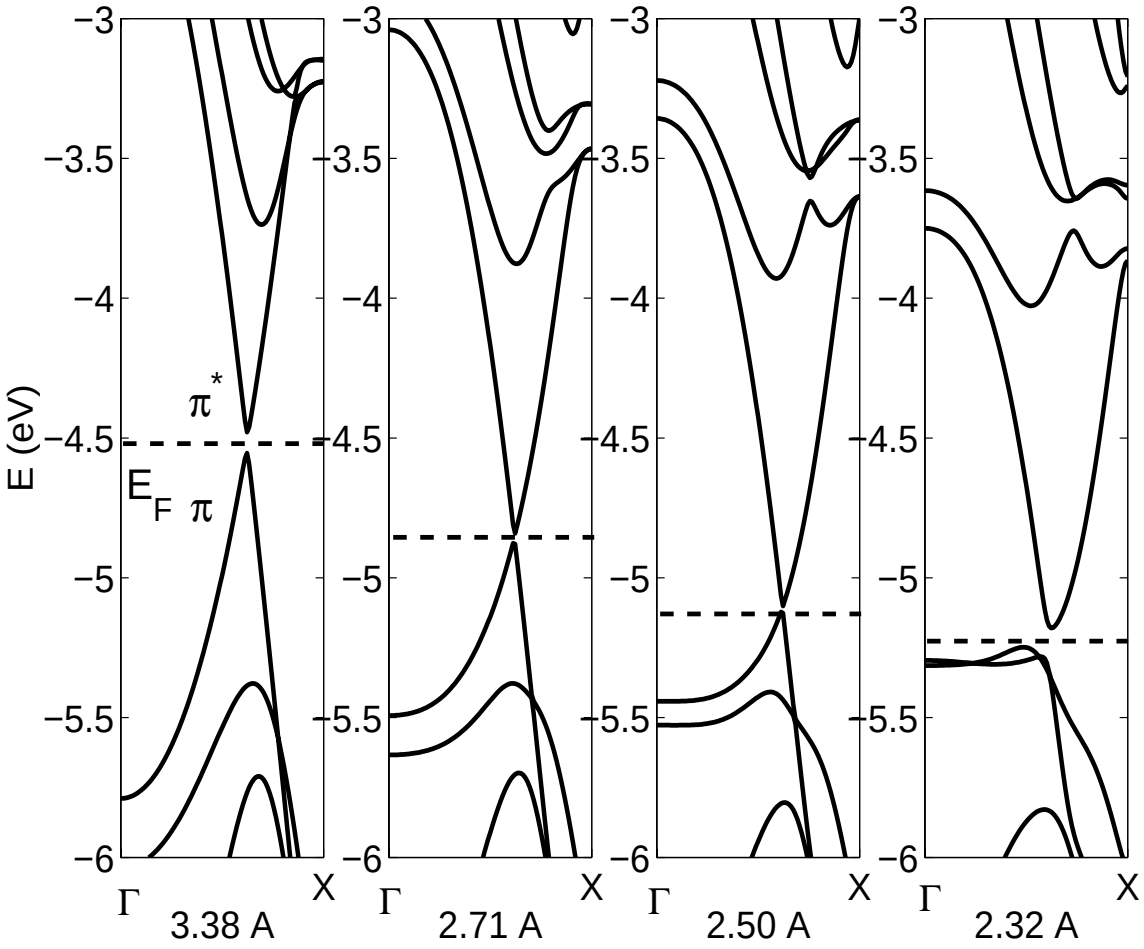

Fig. 5

Svizhenko, Mehrez,Anantram